

Free Vibration Analysis of Composite Laminated Beams

Osama Mohammed Elmardi Suleiman¹, Ahmed F. A. Algarray², and Imad-Eldin Mahmoud Mahdi³

Assistant Professors^{1,3}

Department of Mechanical Engineering,

Faculty of Engineering and Technology,

Nile Valley University, Atbara,

River Nile State,

Sudan

Lecturer²

Department of Mechanical Engineering,

Faculty of Engineering,

Red Sea University, Port Sudan,

Red Sea State,

Sudan

Abstract

This study addresses the problem of free vibration of laminated composite beams. Six end boundary conditions for beams are considered: clamped-clamped; hinged-hinged; free-free; clamped-hinged; clamped-free; and hinged-free beams. The problem is analyzed and solved using the energy approach which is formulated by a finite element model. This method of analysis is verified by comparing the numerical results obtained for AS/3501-6 graphite/epoxy composites with those found in literature. The effects of the aspect ratio, fiber orientation, and the beam end-movements on the non-dimensional natural frequencies of beams were included.

The results of the non-dimensional frequencies for some special cases of lamination were included. The mode shapes of free vibration for all boundary conditions were plotted. It was found that symmetrically $[\theta/-\theta/-\theta/\theta]$ and anti-symmetrically $[\theta/-\theta/\theta/-\theta]$ laminated beams of similar dimensions and end conditions have equal natural frequencies. The longitudinal modes of free vibration are sensitive to axial motion of the ends, whereas the transverse modes depend solely on the condition of the lateral supports. It was also found that natural frequencies decrease as the aspect ratio and/or the angle of orientation increase. The free-free and hinged-free beams are found to have the highest frequencies of all beams although they look less constrained.

Keywords: Laminated beam, finite element, shears deformation, natural frequencies, and free vibration.

1. INTRODUCTION

Composite have been used in engineering structures over the last six decades or so. They could be seen in a variety of applications as in craft wings and fuselage, satellites, helicopter blades, wind turbines, boats and vessels, tubes and

tanks, robot arms, brake pedals and springs etc. Their advantages over traditional materials are widely recognized and these are high strength to weight ratio, and their properties which can be tailored according to need. Other advantages include high stiffness, high fatigue and corrosion resistance, good friction characteristics, and ease of fabrication. They are made of fiber such as glass, carbon, boron, etc. embedded in matrix or suitable resin that acts as binding material. A laminated composite or simply a laminate is a structural element (beam, plate, shell) made up of unidirectional plies stacked together with appropriate orientation that achieve design requirements (see Figure 1).

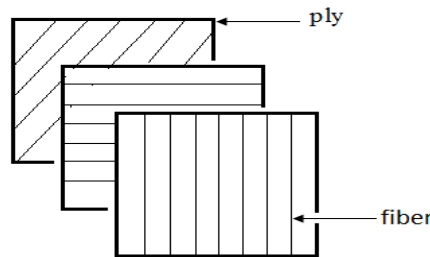


Figure 1 Three plies with their fiber arranged in three different orientations

The ever growing use of composites in industry has led to tremendous advancements in the understanding of their micro and macro behavior. Many mathematical models for laminates subjected to static and dynamic loading have been developed. The knowledge of the few lower natural frequencies of a structure is of utmost importance in order to keep it in service from being subjected to unnecessary large amplitude of motion which can cause immediate collapse or ultimate failure by fatigue.

Broadly speaking the mathematical models for laminates can be divided into three groups depending on whether shear deformation and rotary inertia (in case of vibration) are accounted for or not. Shear deformation is more pronounced in composites than in metals due to low ratio of inter laminar shear modulus to in-plane elastic modulus. The three mathematical models are:

- (i) Classical Laminated Theory (CLT): This theory neglects shear deformation and assumes that sections which are straight and normal to the mid-plane of the laminate remains so after deformation as shown in Figure 2(a). Because shear deformation is neglected, CLT is applicable only to thin laminates. For more information the reader could refer to Abarcar and Cubif [1].
- (ii) First-order Shear Deformation Theory (FSDT): This theory accounts for shear deformation but needs correction. In FSDT, a linear through thickness displacement field is assumed which leads to a constant transverse shear strain or stress that violates the state of zero shear stress on the free surface of the laminate. To reduce error induced by assuming constant rather than parabolic shear stress a shear correction factor is used as suggested by Cowper [2] and Madabhushi & Davalos [3]. The theory is applied by Chen and Yang [4] and Chandrashekhara & Krishnamurthy [5], Mahmoud Yassin and Osama Mohammed Elmardi Suleiman [6] and [7]. The pattern of deformation is given in Figure 2(b).
- (iii) Higher-order Shear Deformation Theory (HSDT): In fact, this is a family of theories rather than one single theory. In HSDT, the stress distribution through thickness accounts for section warping after deformation as seen in Figure 2(c). When displacement through thickness is denoted by u , then according to HSDT:

$$u(x, z) = u(x) + z\phi_1(x) + z^2\phi_2(x) + \dots$$

The number of terms included in the displacement differentiates between different higher-order shear deformations theories. For example see Livingston [8] and Helinger & Reddy [9]. As expected HSDT become more and more complicated, as the number of unknowns increases. Furthermore, HSDT introduces abstract quantities in addition to those which can be physically interpreted.

Comparison between CLT, FSDT and HSDT can be found in Yildirim & Kiral [10] and Song & Waas [9]. It is claimed that the error in CLT is large, and that HSDT is not superior accuracy than FSDT.

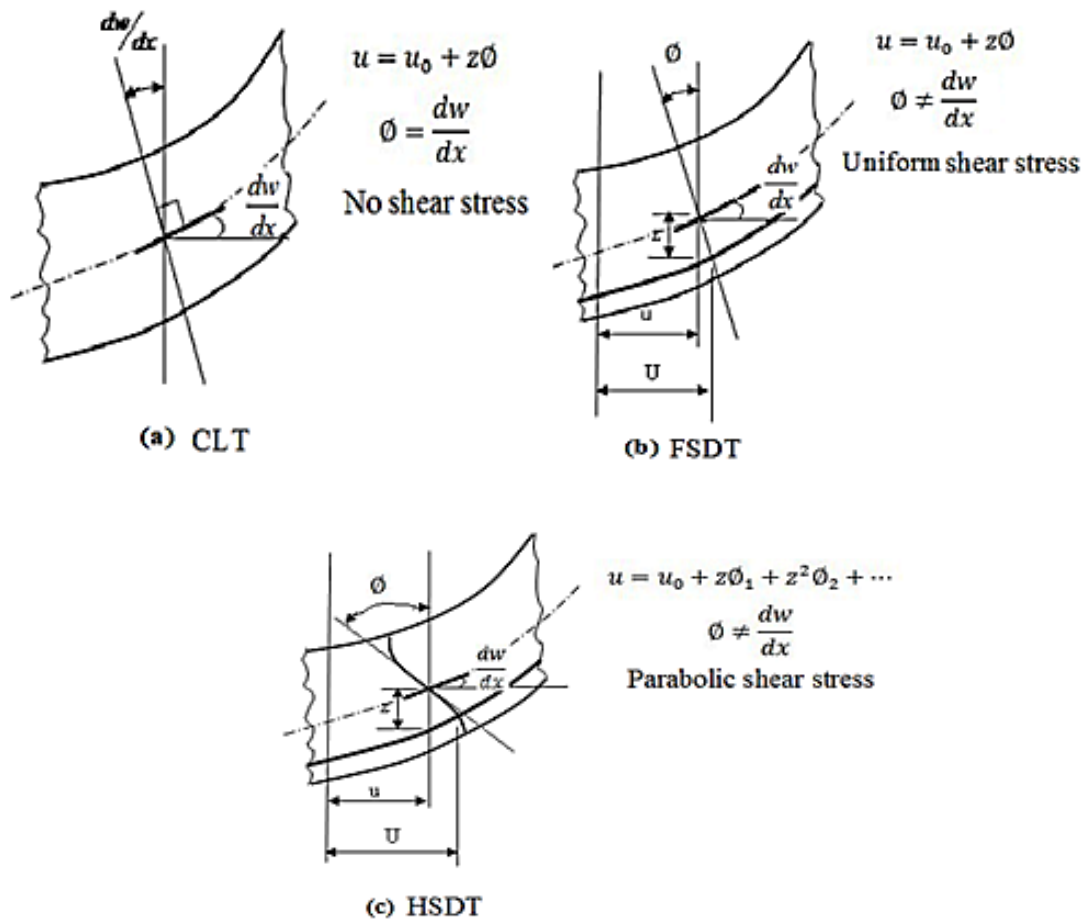


Figure 2 The Three Mathematical Models of Laminated Beams: (a) Deformation of a beam portion according to CLT, (b) Deformation of a beam portion according to FSDT, (c) Deformation of a beam portion according to HSDT

A theoretical vibration analysis of composite beams with solid cross sections was presented by Teoh and Huang [12]. Abramovich [13] studied laminated composite beams considering several boundary conditions. Abramovich and Livshits [14] presented numerical results for the free vibration of a laminated cross-ply composite beams. FSDT was used by Teboub and Hajela [15] to analyze the free vibration of general composite beams, while Ghugal and Shimpi [16] presented a review paper about refined theories for the structural analysis of shear deformable isotropic of laminated beams. Depending on rotary inertia and shear deformation in addition to the coupling between the bending and tensional deformations, the dynamic stiffness matrices have been developed by Banerjee and Williams [17]. Marur and Kant [18] presented the higher order model for the transient dynamic analysis of composite and sandwich beams. Lee [19] presented the natural frequencies for a laminated beam with delimitations (i.e. a beam with defects in

the bonding material between layers). Banerjee [20] added the shape modes of a cantilever composite beam [45/0] to his numerical results.

Some other authors presented different finite element techniques for the problem in addition to the previous ones. These are Subramanian [21], and Yildirim [22]. The latter two authors employed a first order-shear deformation theory, while the former one used a trigonometric shear deformation theory. Matsunaga [23] investigated the natural frequencies, inter-laminar stresses and buckling stresses of composite beams by applying the one-dimensional global higher-order theories that considered the effect of transverse shear deformation. Karama et al. [24] presented a multi-layer laminated composite beam, in this study the exponential function used to predict the mechanical behavior of composite beams. Kapuria et al. [25] assessed a zigzag 1D laminated beam theory and compared the analytical solutions of simply supported beam to the exact 2D elasticity solutions. Murthy et al. [26] supposed a refined 2-node beam element based on the TOSDBT for the free vibration analysis of asymmetrically stacked composite beams. Aydogdu [27] and [28] analyzed the free vibration for cross-ply and angle-ply laminated beams with different boundary conditions. Subramanian [29] developed the free vibration analysis of laminated composite beams applying two higher-order displacement-based shear deformation theories and finite elements based on the theories. Wu and Chen [30] assessed several displacement-based theories by analyzing the free vibration and the buckling behaviors of laminated beams with arbitrary layouts. Vidal and Polit [31] and [32] developed a 3-noded beam element on the basis of a sinus distribution with layer refinement for the dynamic analysis of laminated beams. Vidal and Polit [33] performed the vibration analysis of composite laminated beams by using the Murakami's zigzag function in the sine model. Vo and Thai [34] and [35] presented the free vibration of axially loaded composite beams with arbitrary lay-ups applying the parabolic shear deformation theory. Based on the sinusoidal shear deformation theory, Vo et al. [36] studied the vibration and buckling of composite beams with arbitrary lay-ups. Carrera et al. [37] presented hierarchical beam elements used a unified formulation, where the displacement components were expanded in terms of the section coordinates. On the basis of a unified formulation, Biscani et al. [38] formulated variable kinematics beam elements, which were combined through the Arlequin method. Giunta et al. [39] addressed a free vibration analysis of functionally graded beams via hierarchical models, which were derived via a unified formulation. Giunta et al. [40] presented a unified formulation for the free vibration and elastic stability analysis of three-dimensional sandwich beams, in which shear deformation, in- and out-of-plane warping and rotary inertia were accounted for. Giunta et al. [41] investigated the free vibration of simply supported, cross-ply beams via several higher-order displacement-based theories accounting for non-classical effects. Jun Li et al. [42] compared the various shear deformation theories for free vibration of laminated composite beams with general lay-ups.

2. MODELLING ANALYSIS

Consider a beam of length L , breadth b and depth h made up of n plies with varying thickness, orientation and properties, but perfectly bonded together as shown in Figure 3.

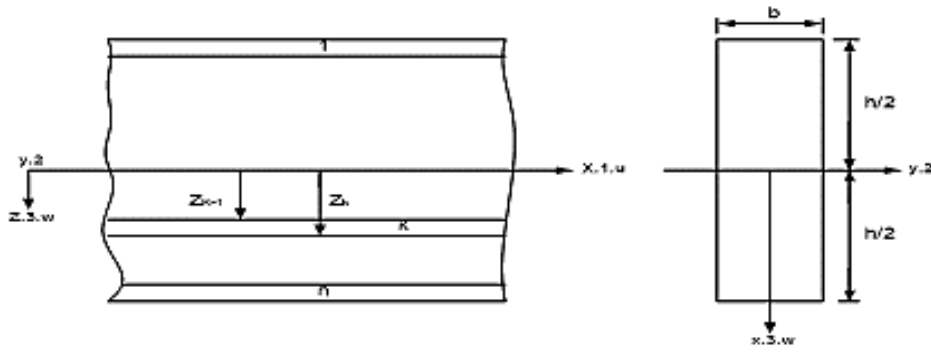


Figure 3 Composite Laminated Beam

Treat the beam as a plane stress problem, and employ first-order shear deformation theory. The longitudinal displacement (U) and the lateral displacement (W) can be written as follows:

$$\left. \begin{aligned} U(x, z, t) &= u(x, t) + z\phi(x, t) \\ W(x, z, t) &= w(x, t) \end{aligned} \right\} (1)$$

Where u and w are the mid-plane longitudinal and lateral displacements, ϕ is the rotation of the deformed section about the y -axis, z is the perpendicular distance from mid-plane to the layer plane, and t is time.

The Strain-Displacement Relations:

$$\left. \begin{aligned} \epsilon_1 &= \frac{\partial U}{\partial x} = \frac{\partial u}{\partial x} + z \frac{\partial \phi}{\partial x} \\ \epsilon_5 &= \frac{\partial W}{\partial x} + \frac{\partial U}{\partial z} = \frac{\partial w}{\partial x} + \phi \end{aligned} \right\} (2)$$

Where: ϵ_1 is the longitudinal strain, and ϵ_5 is the through-thickness shear strain.

By employing 3-noded lineal element as shown in Figure 4:

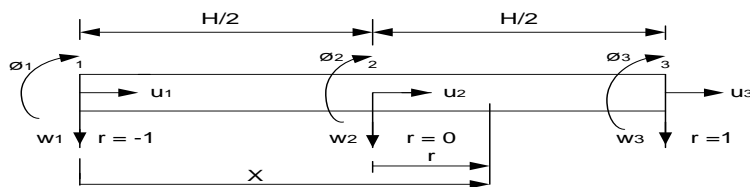


Figure 4 Composite Laminated Beam with 3-Noded Lineal Element

The displacements can be expressed in terms of shape function N_i and nodal displacements:

$$u = N_i u_i \quad , \quad w = N_i w_i \quad , \quad \phi = N_i \phi_i \quad (3)$$

The shape functions are: $N_1 = -\frac{r}{2}(1 - r)$, $N_2 = 1 - r^2$, $N_3 = \frac{r}{2}(1 + r)$

From equations (2) & (3), the strains can be written as: $\epsilon = B a^e$ (4)

Where $B = \begin{bmatrix} \frac{dN_i}{dr} & 0 & z \frac{dN_i}{dr} \\ 0 & \frac{dN_i}{dr} & N_i \end{bmatrix} i = 1,2,3$

And a^e is the vector of nodal displacements $a^e = [u_i \ w_i \ \phi_i]^T i = 1,2,3$

The stress – strain relation: $\sigma = c\epsilon$ (5)

Where $\sigma = [\sigma_1 \ \sigma_5]^T, \epsilon = [\epsilon_1 \ \epsilon_5]^T$ and the matrix containing the transformed elastic constants

$$c = \begin{bmatrix} c_{11} & 0 \\ 0 & c_{55} \end{bmatrix}$$

Substitute equation (4) in equation (5): $\sigma = cBa^e$ (6)

The strain energy: $U_S = \frac{1}{2} \int_V \epsilon^T \sigma dv$ (7)

$$U_S = \frac{1}{2} a^{eT} b \int B^T c B dx dz a^e$$

$$U_S = \frac{1}{2} a^{eT} b K^e a^e \tag{8}$$

Where $K^e = \int B^T c B dx dz$

The kinetic energy: $T = \frac{1}{2} \int \rho [(\dot{u} + z\dot{\phi})^2 + \dot{w}^2] dv$

Where ρ is density and the dot denotes differentiation with time.

$$T = -\omega^2 \frac{a^{eT}}{2} \int \rho N^T Z N a^e dv \quad \text{Or} \quad T = -\frac{1}{2} a^{eT} b \omega^2 M^e a^e \tag{9}$$

Where $M^e = \int \rho N^T Z N dx dz$

$$N = \begin{bmatrix} N_i & 0 & 0 \\ 0 & N_i & 0 \\ 0 & 0 & N_i \end{bmatrix} \& Z = \begin{bmatrix} 1 & 0 & Z \\ 0 & 1 & 0 \\ Z & 0 & Z^2 \end{bmatrix}$$

In the above derivation it is assumed the motion is harmonic and ω is circular frequency.

In the absence of damping and external nodal load, the total energy is: $\mathcal{L} = U_S + T$

Or $\mathcal{L} = \frac{1}{2} a^{eT} b K^e a^e - \frac{1}{2} a^{eT} b \omega^2 M^e a^e$

The principle of minimum energy require that $\frac{\partial \mathcal{L}}{\partial a^e} = 0$

The condition yields the equation of motion

$$K^e a^e - \omega^2 M^e a^e = 0$$

Or globally: $[K - \omega^2 M]a = 0$ (10)

Where

$$K = \sum_{e=1}^n K^e, M = \sum_{e=1}^n M^e, a = \sum_{e=1}^n a^e$$

And n is number of elements. To facilitate the solution of equation (10), we introduce the following quantities:

$$[A_{11}, B_{11}, D_{11}] = \sum_{k=1}^n \int_{Z_{k-1}}^{Z_k} c_{11}[1, Z, Z^2] dz, \quad A_{55} = K_f \sum_{k=1}^n \int_{Z_{k-1}}^{Z_k} c_{55} dz$$

Where K_f is the shear correction factor.

The transformed elastic constants are: $c_{11} = c'_{11}c^4 + 2(c'_{12} + 2c'_{66})S^2C^2 + c'_{22}S^4$

$$c_{55} = c'_{44}S^2 + c'_{55}C^2$$

$$\text{In which: } c'_{11} = \frac{E_1}{1 - \nu_{12}\nu_{21}}, \quad c'_{12} = \frac{\nu_{12}E_2}{1 - \nu_{12}\nu_{21}} = \frac{\nu_{21}E_1}{1 - \nu_{12}\nu_{21}}, \quad c'_{22} = \frac{E_2}{1 - \nu_{12}\nu_{21}}$$

$$c'_{66} = G_{12}, \quad c'_{55} = G_{13}, \quad c'_{44} = G_{23}, \quad S = \sin\theta, \quad C = \cos\theta$$

And θ is the angle of orientation of the ply with respect to the beam axis.

$$[I_1, I_2, I_3] = \sum_{k=1}^n \int_{Z_{k-1}}^{Z_k} \rho[1, Z, Z^2] dz$$

Non-dimensional quantities used in the analysis are:

$$\bar{u} = \left(\frac{L}{h}\right)u, \quad \bar{w} = \frac{w}{h}, \quad \bar{\phi} = \left(\frac{L}{h}\right)\phi, \quad \bar{A}_{11} = \left(\frac{1}{E_1h}\right)A_{11}, \quad \bar{B}_{11} = \left(\frac{1}{E_1h^2}\right)B_{11}, \quad \bar{D}_{11} = \left(\frac{1}{E_1h^3}\right)D_{11}, \quad \bar{A}_{55} = \left(\frac{1}{E_1h}\right)A_{55},$$

$$\bar{I}_1 = \left(\frac{1}{\rho h}\right)I_1, \quad \bar{I}_2 = \left(\frac{1}{\rho h^2}\right)I_2, \quad \bar{I}_3 = \left(\frac{1}{\rho h^3}\right)I_3, \quad \bar{\omega} = \omega \sqrt{\frac{\rho L^4}{E_1 h^2}}$$

The element stiffness matrix: $K^e = \int B^T c B dx dz$

$$K^e = \int \begin{bmatrix} A_{11} \frac{dN_i}{dx} \frac{dN_j}{dx} & 0 & B_{11} \frac{dN_i}{dx} \frac{dN_j}{dx} \\ 0 & A_{55} \frac{dN_i}{dx} \frac{dN_j}{dx} & A_{55} \frac{dN_i}{dx} N_j \\ B_{11} \frac{dN_i}{dx} \frac{dN_j}{dx} & A_{55} N_i \frac{dN_j}{dx} & D_{11} \frac{dN_i}{dx} \frac{dN_j}{dx} + A_{55} N_i N_j \end{bmatrix} dx$$

The stiffness matrix is 9×9 symmetrical matrix. The non-zero non-dimensional element of matrix are:

$$k_{11} = \frac{7n}{3}A_{11}, \quad k_{13} = \frac{7n}{3}B_{11}, \quad k_{14} = \frac{-8n}{3}A_{11}, \quad k_{16} = \frac{-8n}{3}B_{11}, \quad k_{17} = \frac{n}{3}A_{11}, \quad k_{19} = \frac{n}{3}B_{11}$$

$$k_{22} = \frac{7n}{3}\lambda^2 A_{55}, \quad k_{23} = \frac{-\lambda^2}{2}A_{55}, \quad k_{25} = \frac{-8n}{3}\lambda^2 A_{55}, \quad k_{26} = \frac{-2\lambda^2}{3}A_{55}, \quad k_{28} = \frac{n}{3}\lambda^2 A_{55}, \quad k_{29} = \frac{\lambda^2}{6}A_{55}$$

$$\begin{aligned}
 k_{33} &= \frac{7n}{3}D_{11} + \frac{2\lambda^2}{15n}A_{55}, k_{34} = \frac{-8n}{3}B_{11}, k_{35} = \frac{2\lambda^2}{3}A_{55}, k_{36} = \frac{-8n}{3}D_{11} + \frac{\lambda^2}{15n}A_{55}, k_{37} = \frac{-n}{3}B_{11}, k_{38} = \frac{-\lambda^2}{6}A_{55}, \\
 k_{39} &= \frac{n}{3}D_{11} - \frac{\lambda^2}{30n}A_{55}, k_{44} = \frac{16n}{3}A_{11}, k_{46} = \frac{16n}{3}B_{11}, k_{47} = \frac{-8n}{3}A_{11}, k_{49} = \frac{-8n}{3}B_{11}, k_{55} = \frac{16n\lambda^2}{3}A_{55}, \\
 k_{58} &= \frac{-8n\lambda^2}{3}A_{55}, k_{59} = \frac{-2\lambda^2}{3}A_{55}, k_{66} = \frac{16n}{3}D_{11} + \frac{8\lambda^2}{15n}A_{55}, k_{67} = \frac{-8n}{3}B_{11}, k_{68} = \frac{2\lambda^2}{3}A_{55}, k_{69} = \\
 &\frac{-8n}{3}D_{11} + \frac{\lambda^2}{15n}A_{55}, k_{77} = \frac{7n}{3}A_{11}, k_{79} = \frac{7n}{3}B_{11}, k_{88} = \frac{7n\lambda^2}{3}A_{55}, k_{89} = \frac{\lambda^2}{2}A_{55}, k_{99} = \frac{7n}{3}D_{11} + \frac{2\lambda^2}{15n}A_{55}.
 \end{aligned}$$

The mass matrix is 9×9 symmetrical matrix:

$$M^e = \int \rho N^T Z N dx dz, \quad M^e = \int \rho \begin{bmatrix} N_i N_j & 0 & Z N_i N_j \\ 0 & N_i N_j & 0 \\ Z N_i N_j & 0 & Z^2 N_i N_j \end{bmatrix} dx dz, \quad M^e = \int \begin{bmatrix} I_1 N_i N_j & 0 & I_2 N_i N_j \\ 0 & I_1 N_i N_j & 0 \\ I_2 N_i N_j & 0 & I_3 N_i N_j \end{bmatrix} dx$$

The non-zero non-dimensional elements of mass matrix are:

$$\begin{aligned}
 m_{11} &= \frac{2l_1}{2n\lambda^2}, m_{13} = \frac{2l_2}{15n\lambda^2}, m_{14} = \frac{l_1}{15n\lambda^2}, m_{16} = \frac{l_2}{15n\lambda^2}, m_{17} = \frac{-l_1}{30n\lambda^2}, m_{19} = \frac{-l_2}{30n\lambda^2} \\
 m_{22} &= \frac{2l_1}{15n}, m_{25} = \frac{l_1}{15n}, m_{28} = \frac{-l_1}{30n}, m_{33} = \frac{2l_3}{15n\lambda^2}, m_{34} = \frac{l_2}{15n\lambda^2}, m_{36} = \frac{l_3}{15n\lambda^2}, m_{37} = \frac{-l_2}{30n\lambda^2}, \\
 m_{39} &= \frac{-l_3}{30n\lambda^2}, m_{44} = \frac{8l_1}{15n\lambda^2}, m_{46} = \frac{8l_2}{15n\lambda^2}, m_{47} = \frac{l_1}{15n\lambda^2}, m_{49} = \frac{l_2}{15n\lambda^2}, m_{55} = \frac{8l_1}{15n}, m_{58} = \frac{l_1}{15n} \\
 m_{66} &= \frac{8l_3}{15n\lambda^2}, m_{67} = \frac{l_2}{15n\lambda^2}, m_{69} = \frac{l_3}{15n\lambda^2}, m_{77} = \frac{2l_1}{15n\lambda^2}, m_{79} = \frac{2l_2}{15n\lambda^2}, m_{88} = \frac{2l_1}{15n}, m_{99} = \frac{2l_3}{15n\lambda^2}
 \end{aligned}$$

Where $\lambda = \frac{L}{h}$

3. EFFECT OF THE TYPES OF SUPPORT

The numerical results of the non-dimensional natural frequencies of laminated beams, given in this paper, were carried out for six end conditions. The transverse and rotational mode shapes for symmetric angle-ply laminated beams with immovable ends are also displayed in Figure 17 to Fig 20. Moreover, longitudinal mode shapes of some selected non-symmetric laminated beams are given in Figure 21 and Figure 22.

AS/3501-6 graphite-epoxy material was used for all numerical results because of its wide applications in modern industries. The mechanical properties of this material are: $E_1 = 145 \text{ GN/m}^2$, $E_2 = 9.6 \text{ GN/m}^2$, $G_{12} = 4.1 \text{ GN/m}^2$, $G_{13} = 4.1 \text{ GN/m}^2$, $G_{23} = 3.4 \text{ GN/m}^2$, Poisson's ratio $\nu = 0.3$, Density $= 1520 \text{ kg/m}^3$.

3.1 Effect of the Aspect Ratio:

Figure 5 to Figure 10 subjected to symmetric $[45/-45/-45/45]$ angle-ply laminated beams. These figures show the variation of the non-dimensional frequencies with the aspect ratio range from 5 to 40 for the first three modes of vibration for all beams with immovable ends. It is obvious from the figure that the frequency increases rapidly for the

range of aspect ratio from 5 to 20, and slows down beyond this range. When the aspect ratio is greater than 20, the beam is slender and consequently shear deformation and rotary inertia have small noticeable effects on the natural frequencies.

3.2 Effect of Axial Movements of the Ends:

The values of the non-dimensional frequencies of the transverse modes are not affected by the longitudinal movements of the ends since these modes are generated by lateral movements only. However, the values of the natural frequencies of longitudinal modes are found to be the same for all beams with movable ends since they are generated by longitudinal movements only. Table 1, shows this observation for symmetric $[60/-60/-60/60]$ laminated beams with aspect ratio of 10.

Table 1 Non-dimensional natural frequencies $\left[\bar{\omega} = \omega \sqrt{\rho L^4 / E_1 h^2}\right]$ of a symmetric $[60/-60/-60/60]$ laminated beam, ($L/h = 10$).

Mode No.	beam with immovable ends				beam with movable ends					
	CF FF	HH	CC	HC	HF	CF FF	HH	CC	HC	HF
1	0.3596	0.9943	2.0601	1.4899	0.3596	0.9943	2.0601	1.4899		
	1.5370	2.2088			1.5370	2.2088				
2	2.0893	3.6853	5.0523	4.3780	2.0893	3.6853	5.0523	4.3780		
	4.5879	5.5663			4.5879	5.5663				
3	5.3017	7.4807	8.8047	8.1620	5.6426*	5.3017	7.4807	8.8047	8.1620	
	9.8029				8.6142	9.8029				
4	5.6426*	11.2852*	11.2852*	11.2852*	8.6142	9.2760	11.2852*	11.2852*	11.2852*	
	11.2852*				11.2852*	11.2852*				
5	9.2760	11.8779	12.9830	12.4481	11.2852*	11.8779	12.9830	12.4481		
	13.1506	14.4600			13.1506	14.4600				
6	13.6886	16.5673	17.4219	17.0062	13.6886	16.5673	17.4219	17.0062		
	16.9279*	19.2978			17.9208	19.2978				
7	16.9279*	21.3826	22.0152	21.7057	18.3269	21.3826	22.0152	21.7057		
	17.9208	22.5705*			22.5705*	22.5705*				
8	18.3269	22.5705*	22.5705*	22.5705*	22.5705*	22.5705*	22.5705*	22.5705*	22.5705*	
	22.7784	24.1851			22.7784	24.1851				

Notes: The frequencies marked '*' are the modes with predominance of longitudinal vibration.

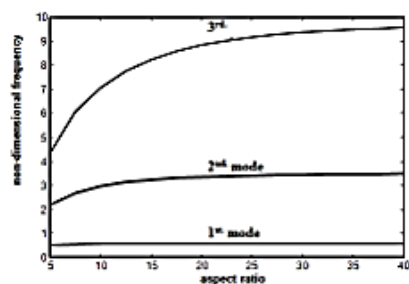


Fig. 5, Effect of aspect ratio on natural frequencies of a symmetric [45/-45/45] cross-ply clamped-free beam

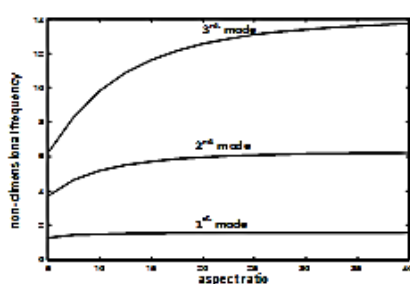


Fig. 6, Effect of aspect ratio on natural frequencies of a symmetric [45/45/-45/45] cross-ply hinged-hinged beam

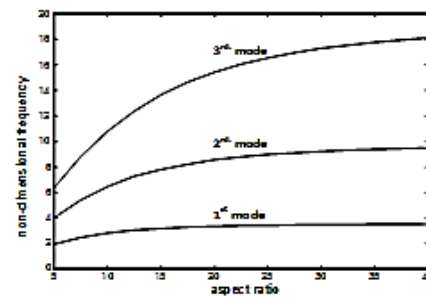


Fig. 7, Effect of aspect ratio on natural frequencies of a symmetric [45/45/-45/45] cross-ply damped-clamped beam

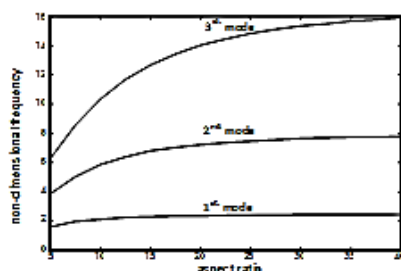


Fig. 8, Effect of aspect ratio on natural frequencies of a symmetric [45/-45/45] cross-ply hinged-clamped beam

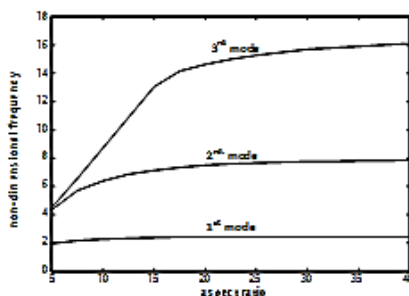


Fig. 9, Effect of aspect ratio on natural frequencies of a symmetric [45/-45/-45/45] cross-ply hinged-free beam

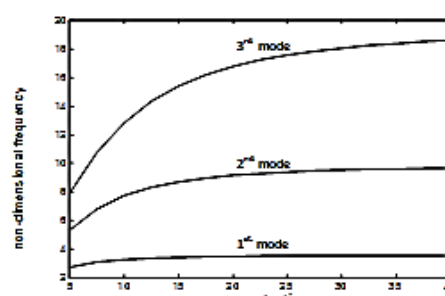


Fig. 10, Effect of aspect ratio on natural frequencies of a symmetric [45/-45/45] cross-ply free-free beam

3.3 Effect of Fiber Orientations:

Figure 11 to Figure 16 show that the values of non-dimensional natural frequencies of various beams generally decrease as the angle of orientation of fibers with respect to the longitudinal axis of the beam is increased.

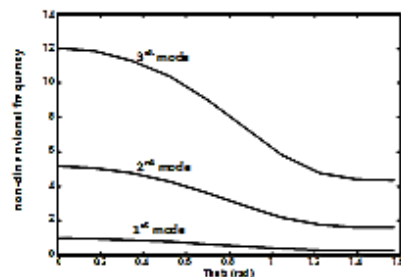


Fig. 11, Effect of angle of orientation on natural frequencies of a symmetric $[\theta/-\theta/-\theta/\theta]$ cross-ply clamped-free beam. $\frac{L}{h} = 10$

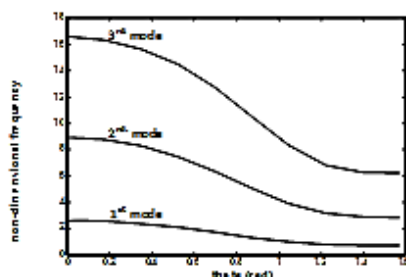


Fig. 12, Effect of angle of orientation on natural frequencies of a symmetric $[\theta/-\theta/-\theta/\theta]$ cross-ply hinged-hinged beam. $\frac{L}{h} = 10$

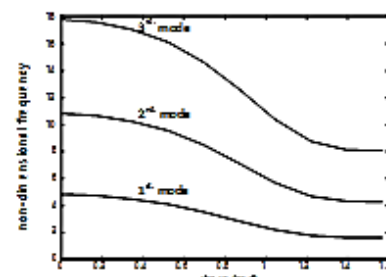


Fig. 13, Effect of angle of orientation on natural frequencies of a symmetric $[\theta/-\theta/-\theta/\theta]$ cross-ply damped-clamped beam. $\frac{L}{h} = 10$

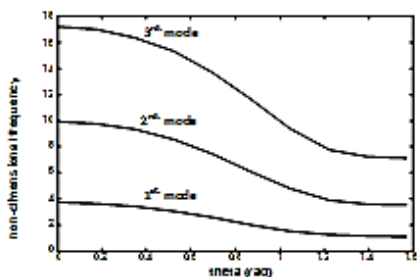


Fig. 14, Effect of angle of orientation on natural frequencies of a symmetric $[\theta/-\theta/-\theta/\theta]$ cross-ply hinged-clamped beam. $\frac{L}{h} = 10$

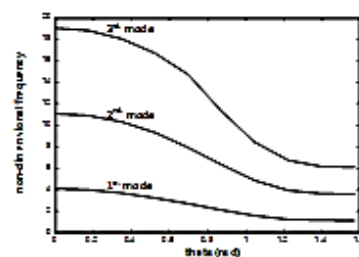


Fig. 15, Effect of angle of orientation on natural frequencies of a symmetric $[\theta/-\theta/-\theta/\theta]$ cross-ply hinged-free beam. $\frac{L}{h} = 10$

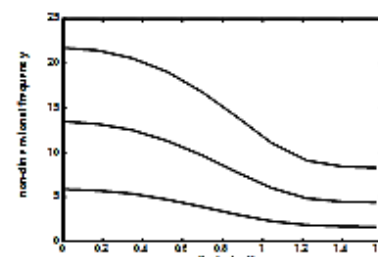


Fig. 16, Effect of angle of orientation on natural frequencies of a symmetric $[\theta/-\theta/-\theta/\theta]$ cross-ply free-free beam. $\frac{L}{h} = 10$

3.4 Effect of the Type of Supports:

The type of supports affects the natural frequencies as could be noted from the table (1). Generally, it is found that more constrained beams have high values of natural frequencies. However, the free-free and hinged-free beams are found to have the highest frequencies amongst all beams although they look less constrained. This behavior is due the fact that the first mode of the two beams is equal zero and replaced by the second mode as could be seen in Figure 21 and Figure 22. The fundamental mode shapes of both beams are straight lines and this due to the rigid motion in this mode where there is no vibrating motion.

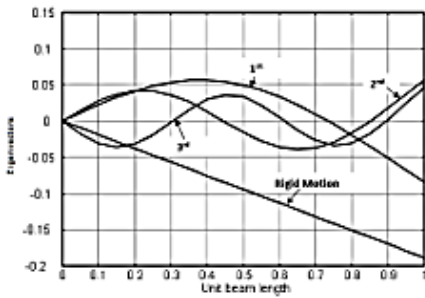


Fig. 8.17, Transverse mode shapes of a symmetric [60/-60/60/60] angle-ply hinged-free beam, L/h=10

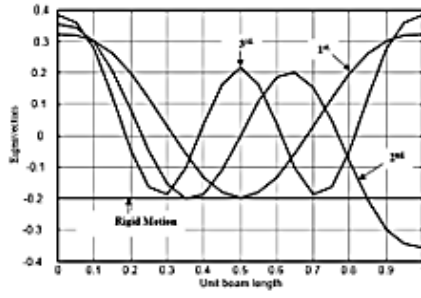


Fig. 18, Transverse mode shapes of a symmetric [60-60/-60/60] angle-ply free-free beam, L/h=10

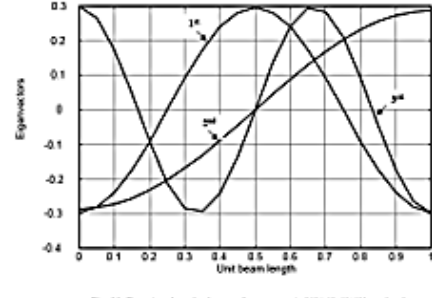


Fig. 19, Rotational mode shapes of a symmetric [60-60-60/60] angle-ply hinged-hinged beam, L/h=10

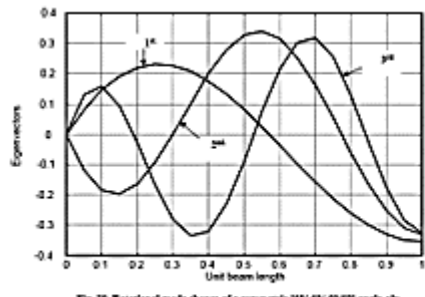


Fig. 20, Rotational mode shapes of a symmetric [60-60-60/60] angle-ply clamped-hinged beam, L/h=10

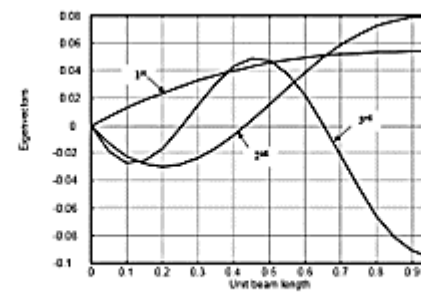


Fig. 21, Longitudinal mode shapes of a non-symmetric [90 0] angle-ply clamped-free beam, L/h=10

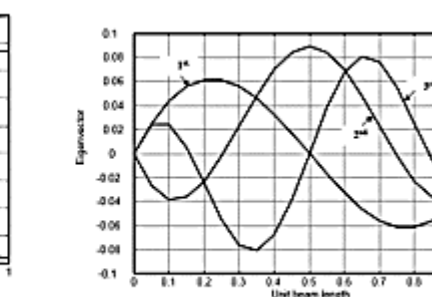


Fig. 22, Longitudinal mode shapes of a non-symmetric [60 0] angle-ply clamped-clamped beam, L/h=10

3.5 Verification:

In order to check the validity of the present method, comparisons with the results of three references [13], [14] and [18] were performed. These comparisons were selected to cover four cases, orthotropic beams, symmetrically laminated beams, non-symmetrically laminated beams, and for different shear theories.

3.5.1 Orthotropic Beams:

Table 2 shows comparison with Abramovich[13]. This comparison shows the first five modes of natural frequencies in (kHz) of simply supported orthotropic ($\theta = 0$) graphite-epoxy beams ($L = 15$ in., $b = h = 1.0$ in.).

Table 2 Natural frequencies of a simply supported orthotropic (0°) graphite-epoxy beam ($L = 15$ in, $h = 1$ in, $w = 1$ in).

Natural frequencies (kHz)							
Mode	Present work				Ref. [11]		
No.	Shear factor, $K_f=2/3$	Shear factor, $K_f=5/6$	Shear factor, $K_s=2/3$	Shear factor, $K_s=5/6$	Shear factor, $K_s=2/3$	Shear factor, $K_s=5/6$	Shear factor, $K_s=5/6$
1	0.000	0.000	0.000	0.000	0.000	0.000	0.000
2	0.000	0.000	0.000	0.000	0.000	0.000	0.000
3	0.000	0.000	0.000	0.000	0.000	0.000	0.000
4	0.000	0.000	0.000	0.000	0.000	0.000	0.000
5	0.000	0.000	0.000	0.000	0.000	0.000	0.000

1	0.7421	0.7544	0.743	0.755
2	2.4300	2.5430	2.431	2.543
3	4.3984	4.7059	4.393	4.697
4	6.4064	6.9514	6.383	6.919
5	8.4082	9.2044	8.349	9.127

When ($K_f = 2/3$), the maximum percentage difference was found to be less than 0.13% for the fundamental frequencies, and 0.70% for the fifth mode. For the second value of the shear correction factor, ($K_f = 5/6$), a percentage difference of less than 0.08% was recorded for the fundamental mode, whereas, a difference of less than 0.80% have been recorded for the fifth mode. Those differences arise because the term representing the joint action of the shear deformation and rotary inertia in the equation of motion has been omitted in Ref. [13] because it is thought to be negligible.

3.5.2 Symmetrically Laminated Beams:

Table 3 presents a comparison with Abramovich and Livshits [14] of the non-dimensional frequencies of symmetric [0/90/90/0] cross-ply graphite-epoxy beams for aspect ratio of ($L/h = 10$). The beams considered are hinged-hinged, fixed-free, and fixed-fixed with immovable ends. Here, the authors introduced the secondary effect of coupling between bending and torsion in their analysis, which is small, compared with the other secondary effects.

Table 3 Non-dimensional frequencies [$\bar{\omega} = \omega.L^2 \sqrt{\rho/E_1 h^2}$] of symmetric [0/90/90/0] cross-ply beams ($L/h = 10$).

Mode No.	Hinged-hinged (Immovable)		Fixed-free (Immovable)		Fixed-fixed (Immovable)	
	Present	Ref. [12]	Present	Ref. [12]	Present	Ref. [12]
1	2.3157	2.3194	0.8866	0.8819	3.6855	3.7576
2	6.9813	7.0029	4.1062	4.0259	7.7244	7.8718
3	12.004	12.037	8.9536	9.1085	12.381	12.573
4	17.010	17.015	11.504*	12.193*	17.192	17.373
5	22.015	21.907	13.924	14.080	22.119	22.200
6	23.007*	23.007*	18.980	18.980	23.007*	23.007*
7	27.094	27.094	24.037	24.037	27.125	27.125

(*) Modes with predominance of longitudinal vibration.

For the hinged-hinged beam, a percentage difference of less than 0.16% recorded for the fundamental frequency, and less than 0.54% for both fixed-free and fixed-fixed beams. This difference was observed to increase as the mode order increases (less than 1.4%) for the seventh mode for all beams considered. In addition, Table 3 shows the modes with predominance of longitudinal vibration.

3.5.3 Non-symmetrically laminated Beams:

Three comparisons with Abramovich and Livshits [14] were given in the Table 4. These tables compare the non-dimensional frequencies of non-symmetric laminated hinged-hinged and clamped-clamped beams respectively for both conditions of movable and immovable ends.

The percentage difference of the frequencies found less than 0.6% for fundamental modes for both movable and immovable ends of hinged-hinged beams, and less than 1.8% for higher modes. For the mode with predominance of longitudinal vibration, the observed difference was less than 0.7% for both conditions as could be seen in Table 4.

Table 4 Non-dimensional frequencies [$p = \omega.L^2 \sqrt{I_1/D}$] of non-symmetrical [90/0] laminated beam ($L/h = 10$) for a hinged-hinged condition.

Mode No.	Immovable ends		Movable ends	
	Present	Ref. [12]	Present	Ref. [12]
1	8.1021	8.1439	6.1110	6.1459
2	21.540	21.661	21.780	21.902
3	43.619	43.778	42.527	42.698
4	63.727	63.787	65.562	65.658
5	88.820	89.150	89.743	86.126
6	89.924*	89.313*	102.22*	102.75*
7	116.27	114.30	114.79	112.80

(*)Modes with predominance of longitudinal vibration.

3.5.4 Different Shear Theories:

Comparison was carried out with the results of Marur and Kant [16]. Table 5 compares the first six modes of the non-dimensional frequencies [$\bar{\omega} = \omega.L^2 \sqrt{\rho/E_1 h^2}$] of symmetric [0/90/90/0] cross-ply, graphite-epoxy, clamped-free beam with aspect ratio of ($L/h = 15$). The authors applied the higher-order shear deformation theory (HOSDT) in the analysis, whereas, the present method uses first-order shear deformation theory. The comparison shows a percentage difference of less than 0.03% for the fundamental mode of vibration. This difference increases with the mode order to less than 3.6% for the sixth mode.

Table 5 Non-dimensional natural frequencies [$\bar{\omega} = \omega.L^2 \sqrt{\rho/E_1 h^2}$] of symmetric [0/90/90/0] cross-ply clamped-free beam. ($L/h = 15$).

Mode No.	Present	Ref. [16]
1	0.9238	0.924
2	4.8886	4.985
3	11.4556	11.832
4	17.2550*	-
5	18.8481	19.573
6	26.7793	27.720

(*)Modes with predominance of longitudinal vibration.

4. CONCLUSIONS

In this paper, free vibration of generally layered composite beams has been studied. Both secondary effects of transverse shear deformation and rotary inertia were included in the analysis. A first-order shear deformation theory was applied in the analysis. A finite element model has been formulated to predict the non-dimensional natural frequencies and to study the influence of both aspect ratio and angle of orientation of fibers on the natural frequencies.

Six end conditions were studied which are clamped-free, hinged-hinged, clamped-clamped, hinged-clamped, hinged-free, and free-free beams with immovable and movable ends.

The main conclusions are:

- (1) Similar beams, which are either, symmetrically laminated $[\theta/-\theta/-\theta/\theta]$, or anti-symmetrically laminated $[\theta/-\theta/\theta/-\theta]$ have equal natural frequencies, also beams of movable and immovable ends have equal values of the transverse natural frequencies. Repetition of a set of layers in symmetric or anti-symmetric similar beams does not alter the natural frequencies of the beam. If the lamination order of a laminated beam is reversed, the natural frequencies will remain the same.
- (2) The ends lateral supports of a beam have a noticeable effect on the longitudinal frequencies of vibration. i.e. All beams with movable ends have equal longitudinal frequencies of vibration, while those of beams with immovable ends are different. Namely, clamped-free and hinged-free beams with immovable ends have equal longitudinal frequencies, and the other beams have also equal longitudinal frequencies.
- (3) The natural frequencies are independent on the breadth of the beam as it cancels out in both stiffness and inertia matrices. It should be noted that treating the beam as a plane stress problem demands that the width must be small compared with the depth.
- (4) The natural frequencies of a laminated beam generally increase with the aspect ratio and they decrease as the fiber orientation angle increases.
- (5) It was found that the more the beam is constrained, the higher are the values of natural frequencies. But, the free-free and hinged-free beams were found to have the highest frequencies amongst all beams in spite they appear to have the least constrains.

REFERENCES

1. Abarcar, R.B. and P.F. Cunniff, The vibration of cantilever beams of fiber reinforced material. *Journal of Composite Materials*, 1972. 6(3): p. 504-517.
2. Cowper, G., The shear coefficient in Timoshenko's beam theory. *Journal of applied mechanics*, 1966. 33(2): p. 335-340.
3. Madabhusi-Raman, P. and J.F. Davalos, Static shear correction factor for laminated rectangular beams. *Composites Part B: Engineering*, 1996. 27(3): p. 285-293.
4. Chen, A.T. and T. Yang, Static and dynamic formulation of a symmetrically laminated beam finite element for a microcomputer. *Journal of Composite Materials*, 1985. 19(5): p. 459-475.
5. Chandrashekhara, K., K. Krishnamurthy, and S. Roy, Free vibration of composite beams including rotary inertia and shear deformation. *Composite Structures*, 1990. 14(4): p. 269-279.
6. Mahmoud Yassin Osman and Osama Mohammed Elmardi Suleiman, Free vibration of laminated plates, *International Journal of Engineering Research and Advanced Technology (IJERAT)*, Vol.03, Issue 4, 2017, p. 31 – 47.

7. Mahmoud Yassin Osman and Osama Mohammed Elmardi Suleiman, Free vibration analysis of laminated composite beams using finite element method, International Journal of Engineering Research and Advanced Technology (IJERAT), Vol.03, Issue 2, 2017, p. 5 – 22.
8. Levinson, M., Further results of a new beam theory. *Journal of Sound and Vibration*, 1981. 77(3): p. 440-444.
9. Heyliger, P. and J. Reddy, A higher order beam finite element for bending and vibration problems. *Journal of sound and vibration*, 1988. 126(2): p. 309-326.
10. Yildırım, V. and E. Kırıl, Investigation of the rotary inertia and shear deformation effects on the out-of-plane bending and torsional natural frequencies of laminated beams. *Composite Structures*, 2000. 49(3): p. 313-320.
11. Song, S. and A. Waas, Effects of shear deformation on buckling and free vibration of laminated composite beams. *Composite Structures*, 1997. 37(1): p. 33-43.
12. Teoh, L. and C.-C. Huang, The vibration of beams of fibre reinforced material. *Journal of Sound and Vibration*, 1977. 51(4): p. 467-473.
13. Abramovich, H., Shear deformation and rotary inertia effects of vibrating composite beams. *Composite Structures*, 1992. 20(3): p. 165-173.
14. Abramovich, H. and A. Livshits, Free vibrations of non-symmetric cross-ply laminated composite beams. *Journal of sound and vibration*, 1994. 176(5): p. 597-612.
15. Teboub, Y. and P. Hajela, Free vibration of generally layered composite beams using symbolic computations. *Composite structures*, 1995. 33(3): p. 123-134.
16. Ghugal, Y. and R. Shimpi, A review of refined shear deformation theories for isotropic and anisotropic laminated beams. *Journal of reinforced plastics and composites*, 2001. 20(3): p. 255-272.
17. Bannerjee, J. and F. Williams, Exact dynamic stiffness matrix for composite Timoshenko beams with applications. *Journal of sound and vibration*, 1996. 194(4): p. 573-585.
18. Marur, S.R. and T. Kant, Transient dynamics of laminated beams: an evaluation with a higher-order refined theory. *Composite structures*, 1998. 41(1): p. 1-11.
19. Lee, J., Free vibration analysis of delaminated composite beams. *Computers & Structures*, 2000. 74(2): p. 121-129.
20. Banerjee, J., Explicit analytical expressions for frequency equation and mode shapes of composite beams. *International Journal of Solids and Structures*, 2001. 38(14): p. 2415-2426.
21. Subramanian, P., Flexural analysis of symmetric laminated composite beams using C 1 finite element. *Composite structures*, 2001. 54(1): p. 121-126.
22. Yildırım, V., Effect of the longitudinal to transverse moduli ratio on the in-plane natural frequencies of symmetric cross-ply laminated beams by the stiffness method. *Composite structures*, 2000. 50(3): p. 319-326.
23. Matsunaga, H., Vibration and buckling of multilayered composite beams according to higher order deformation theories. *Journal of Sound and Vibration*, 2001. 246(1): p. 47-62.

24. Karama, M., K. Afaq, and S. Mistou, Mechanical behaviour of laminated composite beam by the new multi-layered laminated composite structures model with transverse shear stress continuity. *International Journal of Solids and Structures*, 2003. 40(6): p. 1525-1546.
25. Kapuria, S., P. Dumir, and N. Jain, Assessment of zigzag theory for static loading, buckling, free and forced response of composite and sandwich beams. *Composite structures*, 2004. 64(3): p. 317-327.
26. Murthy, M., et al., A refined higher order finite element for asymmetric composite beams. *Composite Structures*, 2005. 67(1): p. 27-35.
27. Aydogdu, M., Vibration analysis of cross-ply laminated beams with general boundary conditions by Ritz method. *International Journal of Mechanical Sciences*, 2005. 47(11): p. 1740-1755.
28. Aydogdu, M., Free vibration analysis of angle-ply laminated beams with general boundary conditions. *Journal of reinforced plastics and composites*, 2006. 25(15): p. 1571-1583.
29. Subramanian, P., Dynamic analysis of laminated composite beams using higher order theories and finite elements. *Composite Structures*, 2006. 73(3): p. 342-353.
30. Zhen, W. and C. Wanji, An assessment of several displacement-based theories for the vibration and stability analysis of laminated composite and sandwich beams. *Composite Structures*, 2008. 84(4): p. 337-349.
31. Vidal, P. and O. Polit, A family of sinus finite elements for the analysis of rectangular laminated beams. *Composite Structures*, 2008. 84(1): p. 56-72.
32. Vidal, P. and O. Polit, Vibration of multilayered beams using sinus finite elements with transverse normal stress. *Composite Structures*, 2010. 92(6): p. 1524-1534.
33. Vidal, P. and O. Polit, A sine finite element using a zig-zag function for the analysis of laminated composite beams. *Composites Part B: Engineering*, 2011. 42(6): p. 1671-1682.
34. Vo, T.P. and H.-T. Thai, Free vibration of axially loaded rectangular composite beams using refined shear deformation theory. *Composite Structures*, 2012. 94(11): p. 3379-3387.
35. Vo, T.P. and H.-T. Thai, Vibration and buckling of composite beams using refined shear deformation theory. *International Journal of Mechanical Sciences*, 2012. 62(1): p. 67-76.
36. Vo, T.P., H.-T. Thai, and F. Inam, Axial-flexural coupled vibration and buckling of composite beams using sinusoidal shear deformation theory. *Archive of Applied Mechanics*, 2013. 83(4): p. 605-622.
37. Carrera, E., et al., Refined beam elements with arbitrary cross-section geometries. *Computers & structures*, 2010. 88(5): p. 283-293.
38. Biscani, F., et al., Variable kinematic beam elements coupled via Arlequin method. *Composite Structures*, 2011. 93(2): p. 697-708.
39. Giunta, G., et al., Hierarchical theories for the free vibration analysis of functionally graded beams. *Composite Structures*, 2011. 94(1): p. 68-74.

40. Giunta, G., et al., Free vibration and stability analysis of three-dimensional sandwich beams via hierarchical models. *Composites Part B: Engineering*, 2013. 47: p. 326-338.
41. Giunta, G., et al., Free vibration analysis of composite beams via refined theories. *Composites Part B: Engineering*, 2013. 44(1): p. 540-552.
42. Li, J., et al., Comparison of various shear deformation theories for free vibration of laminated composite beams with general lay-ups. *Composite structures*, 2014. 108: p. 767-778.